ISSN 1063-7745, Crystallography Reports, 2006, Vol. 51, No. 1, pp. 16–22. © Pleiades Publishing, Inc., 2006.
Original Russian Text © N.V. Zubkova, D.Yu. Pushcharovskiĭ, Yu.K. Kabalov, S.S. Kazantsev, A.V. Voloshin, 2006, published in Kristallografiya, 2006, Vol. 51, No. 1, pp. 23–29.

STRUCTURE OF INORGANIC COMPOUNDS

Crystal Structure of Holtite II

N. V. Zubkova*, D. Yu. Pushcharovskiĭ*, Yu. K. Kabalov*, S. S. Kazantsev, and A. V. Voloshin*****

** Faculty of Geology, Moscow State University, Vorob'evy gory, Moscow, 119992 Russia*
e-mail: dmitp@geol.msu.ru
*** Shubnikov Institute of Crystallography, Russian Academy of Sciences, Leninskiĭ pr. 59, Moscow, 119333 Russia*
**** Geological Institute, Kola Science Center, Russian Academy of Sciences, ul. Fersmana 14, Apatity, 184209 Russia*

Received March 23, 2005

Abstract—The crystal structure of the As-containing mineral holtite II was refined by the Rietveld method. The orthorhombic unit-cell parameters are $a = 4.6893(1)$ Å, $b = 11.881(1)$ Å, $c = 20.394(1)$ Å, sp. gr. *Pnma*, $Z = 4$. Holtite II has an octahedral framework structure composed of two types of nonequivalent columns of Al octahedra, which was found in the structures of dumortierite-group minerals and holtite I. The differences in the structures of holtite II and holtite I were revealed. These differences are associated with the differences in the composition and configuration of the columns of Al(1) polyhedra, which are located inside the framework and are linked to SiO_4 tetrahedra, as well as with the arrangement of pyramidal SbO_3 groups.

PACS numbers: 61.66. Fn

DOI: 10.1134/S1063774506010044

INTRODUCTION

The results of the X-ray diffraction study of the Al borosilicate dumortierite $(Al,\square)Al_6Si_3O_{12}(O_{2.25}OH_{0.75})(BO_3)$ [1], magnesiodumortierite $(Mg,Ti,\square)(Al,\square)_4(Al,Mg,\square)_2Si_3O_{12.04}(OH)_{2.96}(BO_3)$ [2], and chemically related holtite $(Ta,Al,\square)Al_6(Si,Sb)_3O_{12}(O,OH,\square)_3(BO_3)$ [3, 4] suggested that the structures of this mineralogical groups are based on a stable framework formed by Al octahedra. This framework is composed of two types of columns in which Al octahedra are linked to each other by sharing faces or edges, respectively. In these three structures, triangular BO_3 anions occupy relatively narrow channels of triangular cross section, parallel to the [100] direction. Wide channels of hexagonal cross section are more variable in content. In dumortierite, Al octahedra are located in the middle of these channels. These Al octahedra are linked to the octahedral framework through $[SiO_4]$ tetrahedra. The central Al^{3+} cations in the octahedra randomly occupy their positions (by ~75%). In magnesiodumortierite, these polyhedra are also randomly occupied (by ~69%) by Mg and Ti. The main differences between holtite and dumortierite are associated with the partial replacement of Al with Ta in these octahedra and splitting of two nonequivalent Si positions, both main positions being occupied predominantly by Si atoms, whereas two additional positions are occupied by Sb atoms.

In recent years, the structural fragments of dumortierite-group minerals have been revealed in a large number of minerals and synthetic compounds with different compositions and symmetry. The presence of channels in a framework consisting of columns formed by octahedra is a general feature of these structures. The channels of triangular cross section are occupied by triangular or tetrahedral anions. It should be noted that it is these tubular structural fragments filled with the above anions that can be packed in different ways. Variations in the packing mode can be accompanied by the appearance of wider channels of hexagonal cross section ~4 Å in diameter within an octahedral framework (dumortierite, magnesiodumortierite, holtite, ellenbergerite, phosphoellenbergerite, and ekatite). Such channels impart a microporous character to the mineral structures. In other minerals (holtedahlite and satterlyite), these channels are absent.

Interpretation of the composition of holtite and understanding of its structure became even more difficult after the discovery of localities of the second variety of this mineral in Voron'i Tundry (Kola Peninsula) [5] and, more recently, at the Greenbushes mine (Australia) and in Szklary (Poland) [6]. The main features of the second variety of holtite (named holtite II) distinguishing it from the first variety (named holtite I) are associated with a high antimony content and changes in the X-ray powder diffraction pattern noted in [4]. It was hypothesized that the structural disorder typical of holtite I should be even more pronounced in holtite II [4]. However, it was impossible to verify this hypothesis experimentally because of the lack of high-quality single crystals of holtite II variety. These conditions stimu-

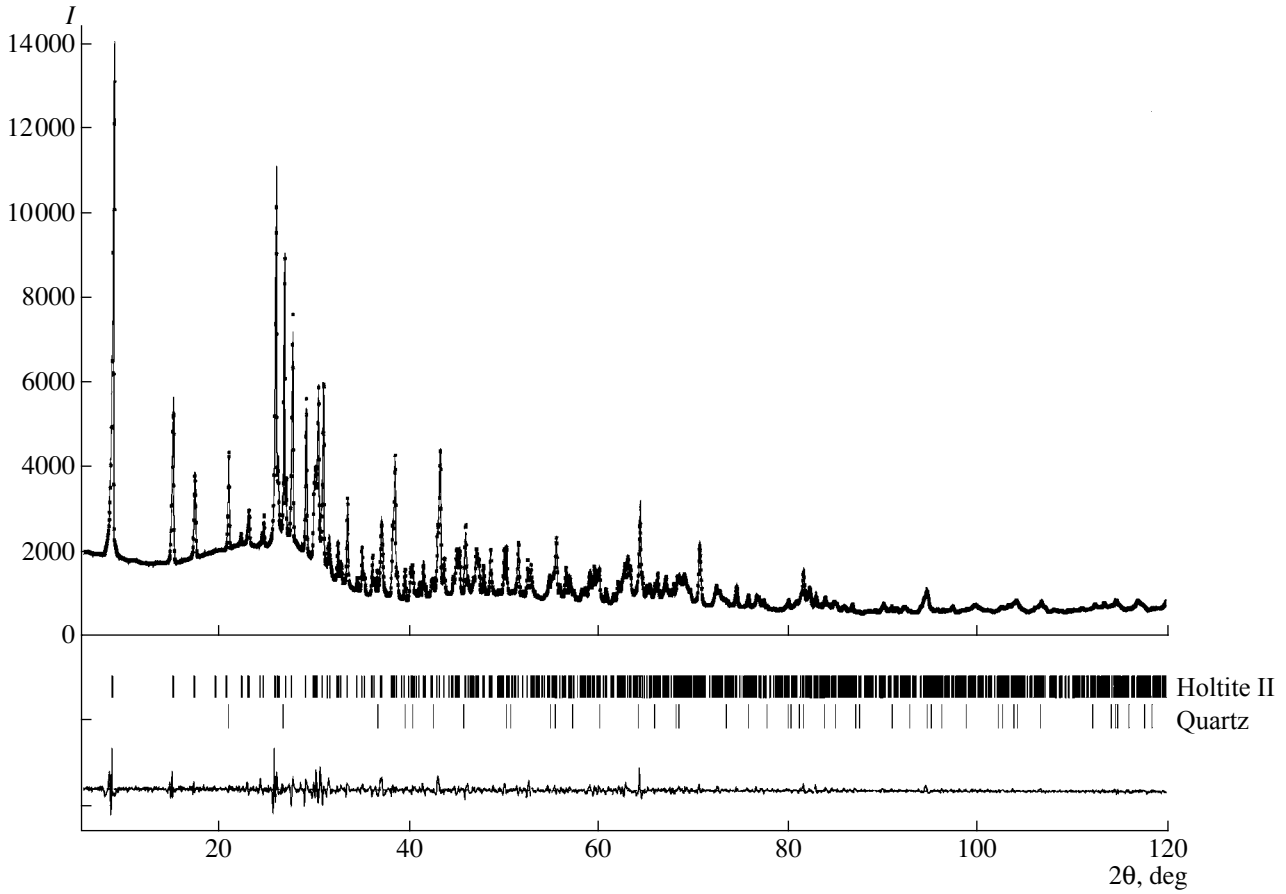

Fig. 1. Theoretical (crosses) and experimental (solid line) X-ray diffraction spectra of a holtite II powder. Vertical bars indicate the positions of all allowed Bragg reflections. The difference spectrum between the observed and calculated spectra is shown by a solid line at the bottom of the figure.

lated investigation of the structure of holtite II by the Rietveld method using polycrystalline samples found in granitic pegmatites from the Kola Peninsula.

EXPERIMENTAL

An X-ray diffraction spectrum of holtite II was measured on a STOE-STADIMP powder diffractometer (curved Ge(111) monochromator, Cu$K_{\alpha 1}$ radiation, λ = 1.54056 Å) equipped with a linear position-sensitive detector in the angle range $5.50° < 2\theta < 120.28°$. A powder sample of holtite II was placed in a 0.3-mm capillary. The X-ray diffraction data were processed using the Wyriet program package (version 3.3) [7]. The structural characteristics were refined using the holtite I structure (sp. gr. *Pnma*) [4] as the starting model. The peak profiles were approximated by the Pearson VII function. Initially, the structural model was fixed and only the scale factor (which brings the observations to an absolute scale), the counter zero, the unit-cell parameters, the peak asymmetry ($2\theta < 57°$), and the peak-widths at half-height were refined using graphical modeling of the background throughout the refinement until the *R* factors ceased to change. In this step, the structural parameters related to a quartz impurity were included in the refinement. The contents of holtite II and quartz in the powder (89.9(1)% and 10.1(1)%, respectively) were estimated by refining the unit-cell volume, the chemical composition, and the scale factor for each phase [8]. In the next step, the following structural parameters were refined: atomic coordinates, isotropic displacement parameters, and occupancies. The refinement of the two-phase sample converged to the following reliability factors (*R* factors): $R_p = \Sigma|I_{obs} - I_{calcd}|/\Sigma|I_{obs}| = 2.93$, $R_{wp} = [\Sigma w|I_{obs} - I_{calcd}|^2/\Sigma w I_{obs}^2]^{1/2} = 3.74$, $GOF = \{\Sigma[w(I_{obs} - I_{calcd})^2]/(N_{obs} - N_{calcd})\}^{1/2} = 1.35$, $R_B = \Sigma|I'_{obs} - I'_{calcd}|/\Sigma I'_{obs} = 2.10$, and $R_F = \Sigma|F_{obs} - F_{calcd}|/\Sigma F_{obs} = 1.88$. The Durbin–Watson statistic *DWD* [9] was 1.10. In these expressions, I'_{obs} and I'_{calcd} are the observed and calculated integrated intensities of Bragg reflections, respectively, and I_{obs} and I_{calcd} are the observed and calculated intensities, respectively. In the final step of structure refinement, the refined values of the unit-cell parameters of holtite II were obtained: a = 4.6893(1) Å, b = 11.881(1) Å, and c = 20.394(1) Å. Figure 1 demonstrates good agreement between the

Table 1. Atomic coordinates, displacement parameters, and occupancies of the positions (Q) in the crystal structure of holtite II

Atom	x	y	z	Q	U_{iso}
Al(1)	0.413(1)	0.75	0.2517(4)	0.30(1) – Ta 0.26(1) – Al	0.019(3)
Al(2)	0.555(2)	0.6080(5)	0.4712(4)	0.95(1) – Al 0.05 – Sb	0.015(4)
Al(3)	0.059(2)	0.4915(7)	0.4320(3)	1	0.009(3)
Al(4)	0.061(2)	0.3604(9)	0.2893(5)	0.98(2)	0.019(4)
Sb(1')	0.103(2)	0.75	0.3911(4)	0.44(1)	0.039(4)
Si(2)	0.586(4)	0.513(2)	0.332(1)	0.65(6)	0.010(2)
Sb(2')	0.619(2)	0.557(1)	0.3192(5)	Sb – 0.30(3) As – 0.05(1)	0.010(2)
O(1)	0.378(5)	0.75	0.454(1)	1	0.001(2)
O(2)	0.165(9)	0.75	0.332(2)	0.56	0.001(2)
O(3)	0.895(4)	0.637(1)	0.4258(7)	1	0.001(2)
O(4)	0.400(4)	0.433(1)	0.2826(7)	1	0.001(2)
O(5)	0.396(4)	0.553(1)	0.3940(7)	1	0.001(2)
O(6)	0.886(4)	0.459(1)	0.3493(7)	1	0.001(2)
O(7)	0.669(5)	0.640(2)	0.290(1)	0.65	0.001(2)
O(8)	0.174(5)	0.25	0.346(1)	1	0.001(2)
O(9)	0.251(3)	0.347(1)	0.4449(9)	1	0.001(2)
O(10)	0.753(4)	0.25	0.280(1)	1	0.001(2)
O(11)	0.746(3)	0.467(1)	0.4893(9)	1	0.001(2)
B	0.23(1)	0.25	0.412(4)	1	0.07(2)

experimental and calculated X-ray diffraction spectra of a powdered mixture of holtite II and quartz.

The structural formula of holtite II determined by refinement is $(Ta_{0.30}Al_{0.26}\square)(Al_{0.95}Sb^{5+}_{0.05})_2Al_2(Al_{0.98}\square)_2 \cdot (Si_{0.65}Sb^{3+}_{0.30}As_{0.05})_2(Sb^{3+}_{0.44}\square)O_{9.30}(O,OH)_{4.56}(BO_3)$, which is, on the whole, in satisfactory agreement with the data from electron-probe analysis: $(Al_{6.40}Ta_{0.36})(Si_{2.11}Sb_{0.97}As_{0.15})O_{12}(O,OH,\square)_3(BO_3)$ [5]. The most significant difference between these formulas is the lower silicon content determined by X-ray diffraction analysis. This discrepancy can be attributed to the fact that the sample that was chemically analyzed contained not only quartz but also amorphous silica, as evidenced by IR spectroscopy. Silica is located between holtite II fibers. Hence, the electron-probe analysis of the mineral overestimated the silica content because the probe diameter is substantially larger that the thickness of fibers in holtite II.

The atomic coordinates, isotropic displacement parameters, and occupancies of the cation positions in the holtite II structure are given in Table 1.

The structure data for holtite II were deposited at the Inorganic Crystal Structure Database (ICSD) with the reference number 415321.

DESCRIPTION AND DISCUSSION OF THE STRUCTURE

The crystal structure of holtite II projected along the [100] direction is shown in Fig. 2. The figure was prepared using the DIAMOND2 program. Holtite II has an octahedral framework structure composed of two types of nonequivalent columns of Al octahedra. This framework was found previously in the structures of dumortierite, magnesiodumortierite, and holtite I [1–4]. In one type of columns, pairs of equivalent Al(4) octahedra share faces, whereas Al(2) and Al(3) octahedra in the other type of columns are linked to each other by sharing edges. The octahedral framework in the holtite II structure differs substantially from the frameworks in the holtite I and dumortierite structures in that ~5% of Al atoms in the Al(2) position in holtite II are randomly replaced by Sb^{5+} cations. The presence of a heavier atom in this position is confirmed by the fact that the refinement of the structural model, in which the Al(2) position was filled only with Al atoms even with an occupancy of 100%, led to the negative isotropic thermal parameter for this position. Along with Sb atoms, the Al(2) position can be occupied by Ta cations. However, by analogy with the holtite I structure, all Ta cations in holtite II were placed in the position Al(1) = (Ta,Al). Both in the holtite I and holtite II structures,

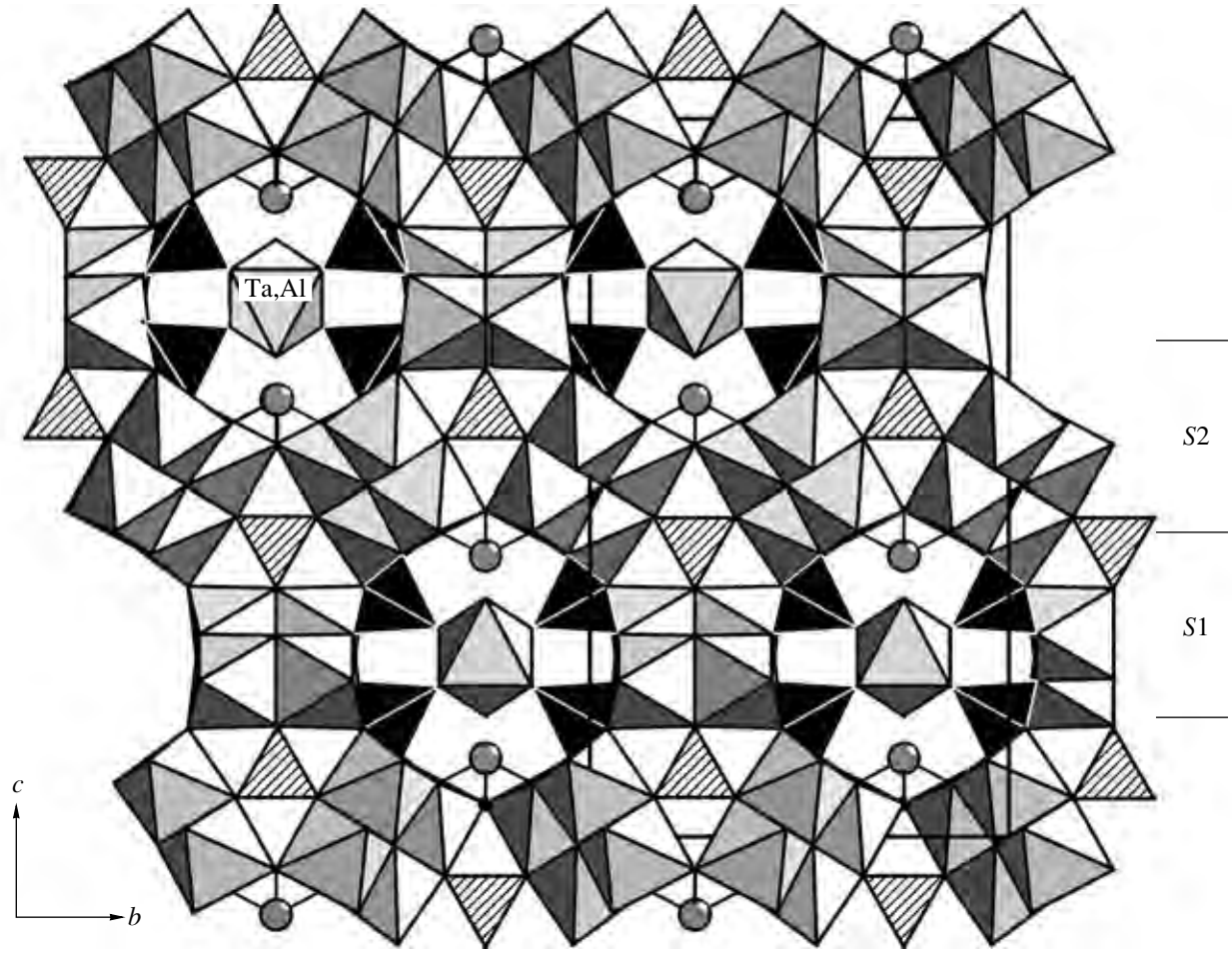

Fig. 2. Crystal structure of holtite II projected along the [100] direction. Aluminum and (Ta,Al) polyhedra are shaded gray, the SiO_4 tetrahedra are black, the BO_3 triangles are diagonally hatched, and the Sb(1') cations are shown by large gray spheres.

$[BO_3]^{3-}$ anions occupy narrower channels of triangular cross section formed by Al octahedra.

The holtite II structure also differs considerably from the structures of holtite I, dumortierite, and magnesiodumortierite, on the one hand, in the structure and composition of the columns formed by Al(1) octahedra and SiO_4 tetrahedra, which are linked to these octahedra and occupy wide channels of hexagonal cross section, and, on the other hand, in the number of pyramidal SbO_3 groups located in these channels. As in the holtite I structure, the Al atoms in the Al(1) octahedra in holtite II are randomly replaced with Ta atoms, with the latter predominating. It should be noted that the total occupancy of the Al(1) position in holtite I is 0.874 ($Al_{0.616(1)}Ta_{0.258(1)}$) [4], whereas the total occupancy of this position in holtite II decreases to 0.56 (the Al to Ta ratio is approximately 1 : 1 ($Ta_{0.30(1)}Al_{0.26(1)}$). The significantly shorter distances between the adjacent (Ta,Al) atoms in holtite II (2.34 Å) are almost equal to the distances between the Al(1) atoms in the dumortierite structure, a phenomenon which should lead to an increase in the number of vacancies in these polyhedra in the case of a larger average radius of the central cations in the octahedra [10]. The replacement of Al with Ta in this octahedron is confirmed by the increase in the central cation–oxygen distances (1.97 Å) in comparison with the Al–O distances in three other Al octahedra (1.91 Å). Even more significant differences in the structure of holtite II, in comparison with that of holtite I, are observed for the Si and Sb^{3+} positions. In the holtite I structure, the positions of two nonequivalent $(Si,As)O_4$ tetrahedra are split [4] and both additional positions are occupied by SbO_3 groups. The occupancies of the (Si,As(1)) and Sb(1') positions are 0.90 and 0.10, respectively. The occupancies of the (Si,As(2)) and Sb(2') positions are 0.87 and 0.13, respectively. The (Si,As(1)) position in the holtite II structure is vacant, whereas this is the main position in holtite I. Only the Sb(1') positions with a coordination number of 3 and occupancy of 0.44(1) were revealed in holtite II. The composition of the (Si,As(2)) position in holtite II also differs significantly from that in holtite I. The occupancy of the Si(2) position is 0.65, and the Sb atoms, together with As atoms, occupy the additional Sb(2')

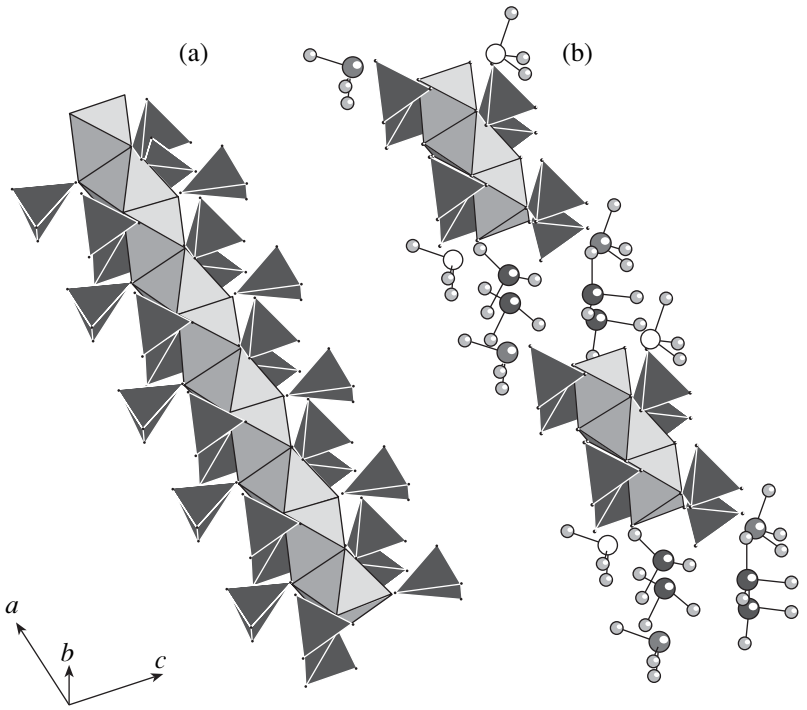

Fig. 3. (a) Column formed by Al(1) octahedra and SiO_4 tetrahedra linked to the column in the dumortierite structure and (b) a formalized fragment of this column in the holtite II structure. Al(1) polyhedra are shaded gray and $Si(2)O_4$ tetrahedra are black. The Sb,As(2') and Sb(1') positions are shown by large black and large gray spheres, respectively. The Sb(1') atoms located near the Al(1) octahedron are shown by empty spheres, and the oxygen positions are shown by small gray spheres.

position revealed in the holtite I structure. The total occupancy of the latter is 0.35 ($Sb_{0.30}$, $As_{0.05}$). The above-described cation distribution should be considered as an optimal compromise between the results of chemical analysis and the electron contents of the corresponding positions revealed by X-ray diffraction analysis of the crystal.

Both in the holtite I and holtite II structures, there are vacancies in the O(2) and O(7) positions because the Sb(1') and O(2) atoms, as well as the (Sb,As(2')) and O(7) atoms, cannot simultaneously be present in the structure; otherwise, the distances between these atoms would be shortened (Sb(1')–O(2) = 1.24(6) Å and (Sb,As(2'))–O(7) = 1.18(4) Å). Hence, the occupancies of the O(2) and O(7) positions are 1 – 0.44 = 0.56 and 1 – 0.35 = 0.65, respectively. The O(2) and O(7) atoms are involved in the (Ta,Al) octahedra. It is reasonable that their occupancies are nearly equal to the occupancies of the central (Ta,Al) atoms in the octahedron.

Figure 3a shows the column composed of Al(1) octahedra and SiO_4 tetrahedra linked to this column in the dumortierite structure. A model of a fragment of this column in the holtite II structure, where Al(1) octahedra are absent and only flattened $Sb(1')O_3$ and (Sb,As)(2') pyramids are located, is shown in Fig. 3b. As mentioned above, free O(2) vertices in each triplet of Al polyhedra can be present only if the Sb(1') position is vacant. In the presence of Sb(1') cations, the Al(1) position becomes five-coordinate.

Since there are no Si atoms in the Si(1) position in the holtite II structure, some oxygen atoms (O(1), O(2), and O(3)), which are involved in the tetrahedra around Si(1) atoms in holtite I, should be replaced with (OH) groups and the corresponding positions should be considered as (O,OH). This accounts for a much higher concentration of hydroxyl anions in holtite II in comparison with holtite I. The simultaneous involvement of the $(OH)^-$ and O^{2-} anions in the above-mentioned positions is also confirmed by calculation of the balance of valence forces of the anions [11]. For the O(1), O(2), and O(3) atoms, the sums of valence forces are 1.70, 0.62, and 1.78, respectively. It should be taken into account that the occupancy of the O(2) atoms is much lower than unity (0.56). In addition to these anions, it is also evident that OH groups are involved in the O(10) position, as in all dumortierite-group minerals. The sum of valence forces for this position is 1.38, a result which suggests the simultaneous presence of O and OH anions in this position, with the hydroxyl groups evidently predominating.

The common structural configuration allows one to compare dumortierite-group minerals with a vast family of minerals and synthetic compounds with different compositions. Table 2 contains the chemical formulas, the space groups, and the compositions of the hexago-

Table 2. Minerals and synthetic compounds structurally related to holtite II

Compound	sp. gr.	Composition of hexagonal channels	Composition of trigonal channels	References
Dumortierite $(Al, \square)Al_6Si_3O_{12}(O_{2.25}OH_{0.75})(BO_3)$	*Pmcn*	$(Al, \square)_2(Si_3O_{12})_2$	(BO_3)	[1]
Magnesiodumortierite $(Mg, Ti, \square)(Al, \square)_4(Al, Mg, \square)_2Si_3O_{12.04}(OH)_{2.96}(BO_3)$	*Pmcn*	$(Mg, Ti, \square)_2 (Si_3O_{12})_2$	(BO_3)	[2]
Holtite I $(Al, Ta, \square)(Al, \square)_6(Si, Sb, As)_3O_{13.43}(O, OH)(BO_3)$	*Pnma*	$(Al, Ta, \square)_2[(Si, Sb, As)_3O_{12}]_2$	(BO_3)	[4]
Holtite II $(Ta, Al, \square)(Al, Sb)_2Al_2(Al, \square)_2(Si, Sb, As)_2(Sb, \square)O_{9.30}(O, OH)_{4.56}(BO_3)$	*Pnma*	$(Ta, Al, \square)_2[(Si, Sb, As)_2(Sb\square)O_{7.3}(O, OH)_{3.56}]_2$	(BO_3)	this study
Ellenbergerite $(Mg, Ti, \square)_2Mg_6Al_6(Si_3O_{12})_2[SiO_3(OH)]_2(OH)_8$	$P6_3$	$(Mg, Ti, \square)_2(Si_3O_{12})_2$	(SiO_3OH)	[12]
Phosphoellenbergerite $Mg_{14}(PO_4)_6[(HPO_4)_{1.24}(CO_3)_{0.76}](OH)_6$	$P6_3mc$	$Mg_2(PO_4)_6$	$[(PO_3OH)_{0.62}(CO_3)_{0.38}]$	[13]
Ekatite $(Fe^{3+}, Fe^{2+}, Zn)_{12}[AsO_3]_6[AsO_3, HOSiO_3]_2(OH)_6$	$P6_3mc$	$(AsO_3)_6$	$[AsO_3, HOSiO_3]$	[14]
Holtedahlite $Mg_{12}(PO_3OH, CO_3)(PO_4)_5(OH, O)_6$	$P31m$	hexagonal channels are absent	(PO_3OH, CO_3)	[15]
$Mg_{12}(PO_3OH)(PO_4)_5(OH, O)_6$ (a synthetic analog)			(PO_3OH)	
Satterlyite $(Fe^{2+}, Mg, Mn)_{12}(PO_3OH)(PO_4)_5(OH, O)_6$	$P31m$	hexagonal channels are absent	(PO_3OH)	[16]
$M_{12}(OH)_2(SeO_3)_8(OH)_6$ (M = Co, Ni)	$P6_3mc$	$(SeO_3)_6(OH)_2$	(SeO_3)	[17]
$M_{11}(HPO_3)_8(OH)_6$ (M = Fe, Mn, Zn, Co, Ni)	$P6_3mc$	$(HPO_3)_6$	(HPO_3)	[18–20]
$Zn_7(OH)_3(SO_4)(VO_4)_3$	$P6_3mc$	$Zn_2(VO_4)_6$	(SO_4)	[21]
$M_3(OH)_2(TeO_3)_2$ (M = Co, Ni)	$P6_3mc$	$(TeO_3)_6(OH)_2$	(TeO_3)	[22]

nal and trigonal channels for various representatives of this family.

The transition from dumortierite and magnesiodumortierite to holtite I, holtite II, and ekatite is clearly seen when considering the compositions of the wide hexagonal channels. In this series, the amount of octahedra located in these channels successively decreases, and the (SiO_4) tetrahedra, through which the octahedra are linked to the framework, are replaced with flattened SbO_3 or AsO_3 pyramids. The main distinguishing feature of ellenbergerite, which is another mineral closely related to both varieties of holtite, is associated with the ordering of two chemically different cations, Mg and Al, in the face-shared octahedra of the framework and the occupation of the octahedra in the middle of the hexagonal channels by Mg and Ti atoms. The structural motifs of synthetic cobalt, zinc, manganese, and iron hydroxy phosphates and nickel and cobalt hydroxy tellurides and hydroxy selenides are analogous to those of the hexagonal minerals ellenbergerite, phosphoellenbergerite, and ekatite.

The structural features of the polyhedral frameworks of hexagonal ellenbergerite and orthorhombic magnesiodumortierite were considered in [2]. The magnesiodumortierite structure was described as containing blocks *S*1 and *S*2 alternating along the [010] direction. Similar blocks can also be distinguished in holtite II and all related structures. One has to take into account that these blocks in holtite II alternate along the [001] direction (Fig. 2) because the *b* and *c* axes in the holtite I and holtite II structures are interchanged. Except for the differences associated with the compositions within the triangular and tetrahedral anions of the framework, the following main features of the hexagonal and orthorhombic dumortierite-related minerals can be distinguished. Blocks *S*1 contain columns, which are composed of face- and edge-shared octahedra (Al(4) in the holtite I and holtite II structures), and octahedra located within wide channels of hexagonal cross section (Al(1) in the holtite I and holtite II structures). The blocks *S*2 in the structures with hexagonal symmetry (ellenbergerite, phosphoellenbergerite, and ekatite) also contain crystallographically equivalent columns formed by face- and edge-shared octahedra. In the structures with orthorhombic symmetry, the octahedra in these channels in blocks *S*2 share edges and vertices (Al(2) and Al(3) octahedra in holtite I and holtite II). Owing to these differences, the rearrangement of the framework with orthorhombic symmetry into the framework with hexagonal symmetry is far from being simple and evident.

ACKNOWLEDGMENTS

This study was supported by the Russian Foundation for Basic Research (project no. 03-05-64054), a joint grant from the Russian Foundation for Basic Research and the Austrian Exchange Service, Agency for International Cooperation in Education and Research (grant no. 03-05-20011BNTS-a), a Grant of the President of the Russian Federation for Support of Young Russian Scientists and Leading Scientific Schools of the Russian Federation (grant no. MK-1046.2004.5), the Program for Leading Scientific Schools (grant no. NSh-1642.2003.5), and the program "Universities of Russia."

REFERENCES

1. P. M. Moore and T. Araki, Neues Jahrb. Mineral., Abh. **132**, 231 (1978).
2. G. Ferraris, G. Ivaldi, and C. Chopin, Eur. J. Mineral **7**, 167 (1995).
3. B. F. Hoskins, W. G. Mumme, and M. W. Pryce, Mineral. Mag. **53**, 457 (1989).
4. S. S. Kazantsev, D. Yu. Pushcharovskiĭ, M. Pazero, *et al.*, Kristallografiya **50** (1), 49 (2005) [Crystallogr. Rep. **50**, 42 (2005)].
5. A. V. Voloshin, Ya. A. Pakhomovskiĭ, and O. A. Zalkind, in *Mineral Associations and Minerals of Magmatic Complexes of the Kola Peninsula* (Izd-vo KF AN SSSR, 1987), p. 14 [in Russian].
6. L. A. Groat, E. S. Grew, T. S. Ercit, and A. Pieczka, in *Abstracts of the 18th General Meeting of the International Mineralogical Association, Edinburgh, 2002*, p. 209.
7. J. Schneider, in *Proceedings of the International Workshop on the Rietveld Method, Petten, 1989*.
8. D. L. Bish and S. A. Howard, J. Appl. Crystallogr. **21**, 86 (1988).
9. R. J. Hill and H. D. Flack, J. Appl. Crystallogr. **20**, 356 (1987).
10. Y. Fuchs, A. Ertl, J. M. Hughes, *et al.*, Eur. J. Mineral **17**, 173 (2005).
11. N. E. Brese and M. O'Keeffe, Acta Crystallogr., Sect. B: Struct. Sci. **47**, 192 (1991).
12. P. Comodi and P. F. Zanazzi, Eur. J. Mineral **5**, 819 (1993).
13. G. Raade, C. Romming, and O. Medenbach, Mineral. Petrol. **62**, 89 (1998).
14. P. Keller, Eur. J. Mineral **13**, 769 (2001).
15. C. Romming and G. Raade, Mineral. Petrol **40**, 91 (1989).
16. U. Kolitsch, M. Andrut, and G. Giester, Eur. J. Mineral **14**, 127 (2002).
17. P. Amoros, M. D. Marcos, M. Roca, *et al.*, J. Solid State Chem. **126**, 169 (1996).
18. M. P. Attfield, R. E. Morris, and A. K. Cheetham, Acta Crystallogr. **50**, 981 (1994).
19. M. D. Marcos, P. Amoros, and A. Le Bail, J. Solid State Chem. **107**, 250 (1993).
20. M. D. Marcos, P. Amoros, A. Beltran-Porter, *et al.*, Chem. Mater. **5**, 121 (1993).
21. K. Kato, Y. Kanke, Y. Oka, and T. Yao, Z. Kristallogr.–New Cryst. Struct. **213**, 26 (1998).
22. G. Perez, F. Lasserre, J. Moret, and M. Maurin, J. Solid State Chem. **17**, 143 (1976).

Translated by T. Safonova